

Quantum Phase Transition in CeCoIn₅: Experimental Facts and Theory

V. R. Shaginyan,^{1,2,*} A. Z. Msezane,² M. V. Zverev,^{3,4} and Y. S. Leevik⁵

¹*Petersburg Nuclear Physics Institute of NRC "Kurchatov Institute", Gatchina, 188300, Russia*

²*Clark Atlanta University, Atlanta, GA 30314, USA*

³*NRC Kurchatov Institute, Moscow, 123182, Russia*

⁴*Moscow Institute of Physics and Technology, Dolgoprudny, Moscow District 141700, Russia*

⁵*National Research University Higher School of Economics, St.Petersburg, 194100, Russia*

Condensed-matter community is involved in hot debate on the nature of quantum critical points (QCP) governing the low-temperature properties of heavy fermion metals. The smeared jump like behavior revealed both in the residual resistivity ρ_0 and the Hall resistivity R_H , along with the violation of the time invariance symmetry \mathcal{T} and the charge invariance \mathcal{C} , including the violation of quasiparticle-hole symmetry, and providing vital clues on the origin of both the non-Fermi-liquid behavior and QCP. For the first time, based on a number of important experimental data, we show that these experimental observations point out unambiguously that QCP of CeCoIn₅ is accompanied by the symmetry violation, and QCP itself is represented by the topological fermion-condensation quantum phase transition (FCQPT) connecting two Fermi surfaces of different topological charges.

It is accepted that the fundamental physics of heavy fermion (HF) metals is controlled by quantum phase transitions, see e. g. [1–10]. A quantum phase transition could be driven by control parameters such as pressure P , number density x of electrons (holes), magnetic field B , etc, taking place at its quantum critical point (QCP) at zero temperature, $T = 0$. The modern physics of condensed-matter is represented by the experimental discovery of flat bands since HF compounds with flat bands are numerous [11]. As a result, one expects the existence of a general physical mechanism generated by the presence of flat bands, forming the universal properties of HF compounds.

The magnetic field dependence of the Hall coefficient $R_H(B)$ provides information about QCP, determining the properties of HF metals. Experiments have shown that the Hall coefficient $R_H(B)$ in the antiferromagnetic HF metal YbRh₂Si₂ in magnetic fields B undergoes a jump in the zero temperature limit under the application of B tuning the metal from antiferromagnetic to a paramagnetic state at $B = B_{c0}$ [12]. The jump takes place when B reaches the critical value B_{c0} at which the Néel temperature $T_N(B)$ of the antiferromagnetic transition vanishes, $T_N(B \rightarrow B_{c0}) \rightarrow 0$. The jump is interpreted as a collapse of the large Fermi surface precisely at QCP [12]. The fermion condensation (FC) theory successfully explains such types of behavior as both the universal scaling behavior and the transition from the non-Fermi liquid (NFL) state to the Landau Fermi liquid (LFL) one [5, 6, 13]. Moreover, the FC state is characterized by broken \mathcal{T} and \mathcal{C} symmetries [2, 5, 6, 14–16] taking place at the interaction driven topological fermion condensation phase transition (FCQPT) that connects two Fermi surfaces of different topological charges and forms flat bands [1, 5, 8]. Recent measurements on the prototypical HF metal CeCoIn₅ of the Hall coefficient allow one to

interpret the observed quantum phase transition as a delocalization quantum phase transition without symmetry breaking in CeCoIn₅, that is characterized by the delocalization of f -electrons in the transition that connects two Fermi surfaces of different volumes [3].

In this letter, for the first time, based on a number of important experimental data, we reveal the quantum phase transition, that forms the properties of archetypical HF metal CeCoIn₅, being characterized by the presence of flat bands [17] and related to the violation of symmetries. We show that the measured thermodynamic and transport properties yield direct evidence for the apparent broken symmetries like the violation of the \mathcal{T} and \mathcal{C} symmetries taking place at the topological FCQPT that occurs in both the archetypical HF metals CeCoIn₅ and YbRh₂Si₂.

Consider $T - B$ phase diagram of the HF metal CeCoIn₅ with the upper critical field $B_{c2} = 5.1$ T along the [001] direction [18–21]. The application of magnetic field along the [100] direction makes the upper critical field $B_{c2} = 11.8$ T and leads to the complicated superconducting part of the phase diagram [22, 23], that is not related with our consideration of the phase diagram 1 at relatively low magnetic fields. The phase diagram is presented schematically in Fig. 1. The HF metal CeCoIn₅ is a superconductor with $T_c = 2.3$ K with the field tuned QCP occurring at the critical field $B_{c0} \simeq 5.0$ T, while the superconducting critical field $B_{c2} \simeq 5.1$ T. Thus, QCP is hidden by the superconducting state, as seen from Fig. 1. We note that $B_{c0} \simeq B_{c2}$ is an accidental coincidence. Indeed, it is shown that the application of increasing pressure P , QCP moves inside the superconducting dome, thus removing the above coincidence[24].

At temperatures $T \sim 2.3$ K the superconducting-normal phase transition shown by the solid line in Fig. 1 is of the second order [21, 25] and entropy S is continuous at $T_c(B)$. Since $B_{c2} \simeq B_{c0}$, upon the application of magnetic field $B > B_{c2}$, the HF metal transits to its LFL state down to lowest temperatures, as seen from Fig. 1. At $T \rightarrow 0$ the entropy of the superconducting

*Electronic address: vrshag@thd.pnpi.spb.ru

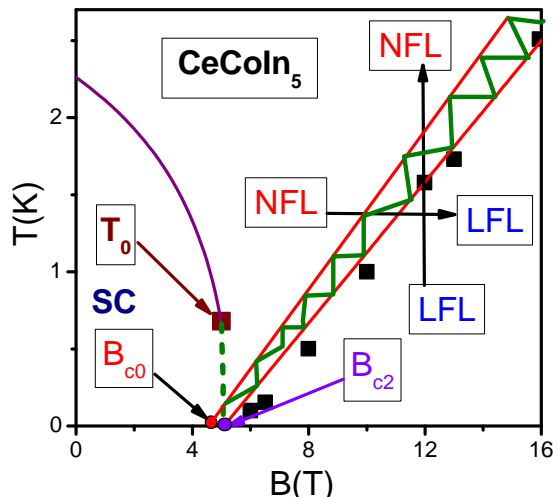


FIG. 1: (color online) Schematic $T - B$ phase diagram of CeCoIn_5 , with the upper critical field $B_{c2} \simeq 5.1$ T along the [001] direction. The vertical and horizontal arrows crossing the transition region are marked by the line depicting the LFL-NFL and NFL-LFL transitions at fixed B and T , respectively. Experimental data obtained from resistivity $\rho(T)$ measurements (upper bound of T^2 resistivity) are shown by the solid squares [19, 20]. The hatched area indicates the crossover from the LFL state, with $\rho(T) \propto T^2$, to NFL one, with $\rho(T) \propto T$. As shown by the solid curve, at $B < B_{c2}$ the system is in its superconducting (SC) state, with B_{c0} denoting QCP hidden beneath the SC dome and shown by the red circle. The superconducting critical field $B_{c2} \simeq 5.1$ T is depicted by the violet circle. Superconducting-normal phase boundary [21] is depicted by the solid and dashed curves. The solid squares show the point at $T = T_0$ where the superconducting phase transition T_c changes from the second to the first order.

state $S_{SC} \rightarrow 0$ and the entropy of the NFL state tends to some finite value $S_{NFL} \rightarrow S_0$ [2], since the ground state of systems with FC is degenerate, and at $T = 0$ the quasiparticle distribution function $n_0(\mathbf{p})$ of flat band is a continuous function in the interval $[0, 1]$, in contrast to the Landau FL restriction on $n_0(\mathbf{p})$ that equals 1 and 0 [13], see Fig. 2. This property leads to the finite value S_0 given by

$$S_0 = - \sum_{\mathbf{p}} n_0(\mathbf{p}) \ln n_0(\mathbf{p}) + (1 - n_0(\mathbf{p})) \ln(1 - n_0(\mathbf{p})). \quad (1)$$

As a result, at sufficiently low temperatures the equality $S_{SC}(T) = S_{NFL}(T)$ cannot be satisfied [5, 26]. In accordance with the experimental observations [21, 25], the second order phase transition converts to the first one below some temperature $T_0(B)$, being related to the flat band, induced by FCQPT, and shown by the arrow in Fig. 1 [26]. Thus, we conclude that the phase transition taking place in CeCoIn_5 is the symmetry breaking, since the FC state with a flat band has the special topological charge different from that of LFL state. In contrast to LFL or marginal liquids which exhibit the same topo-

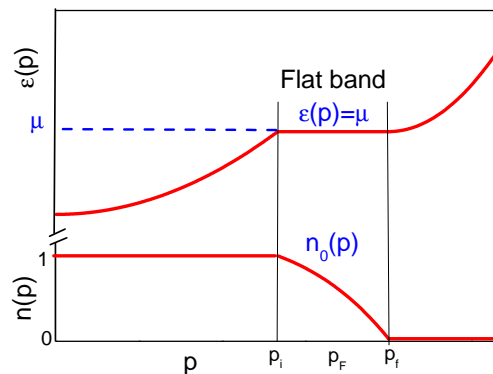


FIG. 2: (color online) The single-particle spectrum $\varepsilon(p)$ and the quasiparticle distribution function $n_0(p)$ of the FC state [5]. Because $n_0(p)$ represents the FC state, we have $n_0(p) = 1$ at $p \leq p_i$, $0 < n_0(p) < 1$ at $p_i < p < p_f$ and $n_0(p) = 0$ at $p \geq p_f$.

logical structure, systems with FC, where the Fermi surface spreads into a strip, belong to a different topological class. In case of LFL or marginal liquids the topological charge takes integer values. The situation is quite different for systems with FC, where the topological charge becomes a half-integer, transforming a system with FC into a new class of Fermi liquids with its own topological structure [2, 8]. The topological FCQPT is of the first order, since the topological charge is changed abruptly. As a result, possible fluctuations of order parameters are suppressed [5].

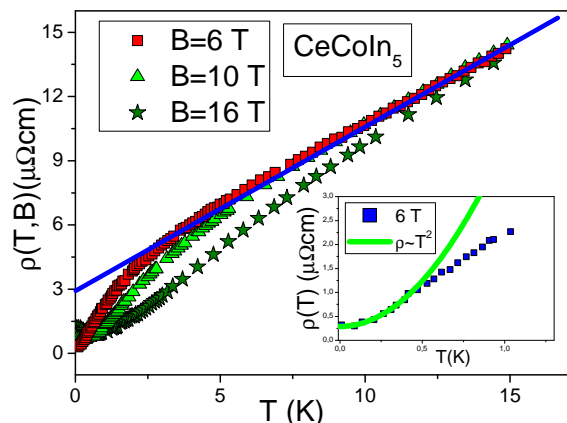


FIG. 3: (color online) Resistivity $\rho(T, B)$ obtained in measurements on CeCoIn_5 under the application of magnetic fields B displayed in the legend [19]. The inset exhibits both the LFL behavior of the resistivity at low temperatures and the crossover with $1 \lesssim n \lesssim 2$ at elevated T .

The resistivity $\rho(T)$ is of the form

$$\rho(T) = \rho_0 + AT^n, \quad (2)$$

where ρ_0 is the residual resistivity and A is a T -independent coefficient. The index n takes the values 1 and 2, respectively, for the NFL and LFL behaviors and

$1 \lesssim n \lesssim 2$ in the NFL-LFL transition, see Figs. 1, 3 and 4 (a). The residual resistivity ρ_0 ordinarily results from impurity scattering [13]. At $T > T_c$ the zero-field resistivity $\rho(T, B = 0)$ varies linearly with T , see Eq. (2). At magnetic fields $B \geq B_{c2}$ and low temperatures the resistivity exhibits the LFL behavior, $\rho(T, B_{c2}) \propto T^2$. Experimentally, CeCoIn₅ is one of the purest heavy-fermion metals. As a result, the regime of electron motion is ballistic. Thus, under the application of weak magnetic field B one expect to observe a small positive contribution $\delta_B \propto B^2$ to ρ_0 arising from orbital motion of electrons induced by the Lorentz force. As seen from Figs. 3 and 4 (a), this is not the case: specifically $\rho_0 \simeq 3.0 \mu\Omega\text{cm}$ in the NFL state, while $\rho_0(B = 6 \text{ T}) \simeq 0.3 \mu\Omega\text{cm}$ in the LFL state, see the inset to Fig. 3, [19, 20], and Fig. 4 (a) [27]. The observed behavior is defined by the destruction of the FC state by magnetic field, while the FC state itself creates the additional residual resistivity [7, 28]. We note, that even the application of strong magnetic fields leads to the negative magnetoresistivity [19], since the effective mass diminishes in magnetic fields, $\rho(B) \propto M^*(B)^2 \propto B^{-4/3}$, [5]. Such a behavior gives the support that CeCoIn₅ is located near the topological FCQPT [5]. Moreover, it is seen from Fig. 3 that at elevated temperatures all the resistivities taken at different fields $B = 6, 10, 16 \text{ T}$ tend to coincide at the NFL state with $\rho(T) \propto T$, since the contribution δ_B is relatively small.

Another direct experimental confirmation of the change of ρ_0 (at the transition from the NFL state to the LFL one) is obtained in measurements on CeCoIn₅ at various pressures P [27]. As seen from Fig. 4 (a), $\rho_0(P \rightarrow 0) \rightarrow 3.0 \mu\Omega\text{cm}$ with $n = 1$, and decreases by an order of magnitude to a value of about $\rho_0(P \geq P^*) \rightarrow 0.2 \mu\Omega\text{cm}$, with $P^* \simeq 1.6 \text{ GPa}$ and $n = 2$ [27]. Note that these values of the residual resistivity coincide with those shown in Fig. 3. Obviously, pressure P does not remove impurities from the sample. Thus, this large decrease in ρ_0 is due to a pressure-induced destruction of the FC state, as seen from the restoration of the LFL behavior at $P \geq P^*$. Similarly, the resistance $\rho(T, B)$ at fixed T as a function of B diminishes when the system transits from the NFL behavior to LFL one under the application of magnetic field (the magnetoresistance becomes negative) [19]. This behavior is consistent with the FC theory [5]. Thus, the destruction of the FC state under the application of both magnetic fields B and pressure P entails a dramatic suppression of the flat band and its contribution to ρ_0 [7, 28]. The same behavior of ρ_0 has been observed on twisted bilayer graphene where strong variation of ρ_0 is seen toward the magic angle [29]. In that case the residual resistivity increases by more than three orders of magnitude and resembles the behavior of ρ_0 shown in Fig. 4 a [7, 28].

Now consider the scattering rate $1/\tau$. In the LFL theory $1/\tau$ is proportional to T^2 , leading to Eq. (2) with $n = 2$. The NFL behavior comes from the NFL temperature dependence of $1/\tau$ associated with the presence of FC [28]. As a result, the scattering rate becomes

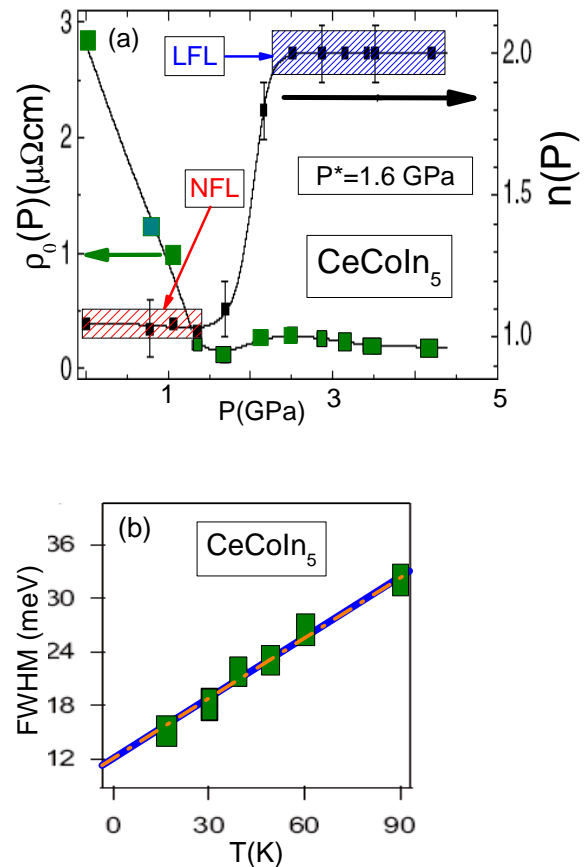


FIG. 4: (color online) Panel (a): Values of the residual resistivity ρ_0 (left axis, solid squares) and the index n in the fit $\rho(T) = \rho_0 + AT^n$ (right axis, solid squares) versus pressure P [27]. At $P < P^*$ CeCoIn₅ is in its NFL state, at $P > P^*$ is in its LFL one, correspondingly. Both the NFL and LFL states are shown by the arrows. Panel (b): Temperature dependence of the full width at half maximum (FWHM) of the single-particle scattering rate of the main Kondo resonance [17] is shown by the solid squares. The line represents the best fit, giving $\text{FWHM} = 11.8 + 2.69Tk_B$ meV, where k_B is the Boltzmann constant [17]. The dash-dot line is the theory [28].

$\hbar/\tau \simeq a_1 + a_2T$ [28]. Here \hbar is Planck's constant, a_1 and a_2 are parameters. This result is in good agreement with experimental facts [17, 30], displayed in Fig. 4 (b). Thus, the FC theory successfully explains the behavior of the scattering rate and $\rho(T) \propto T$ [28]. Taking into account the above consideration of the resistivity behavior, we conclude that QCP in CeCoIn₅ is not related to the delocalization of f -electrons at QCP, since the delocalization is to lead to the suppression of the resistivity $\rho(T)$ and does not change the residual resistivity ρ_0 . While the suppression of ρ_0 takes place when CeCoIn₅ transits from the NFL behavior to LFL one under the application of B or P , see Figs. 3 and 4, and is defined by the destruction of the flat band, accompanied by the change of the topological charge [2, 8].

The presence of the flat band manifests itself not

only in the transport properties, but also in the universal scaling behavior of the thermodynamics properties of HF metals [5, 6]. To elucidate this behavior, we briefly consider the LFL equations defining the effective mass $M^*(T, B)$. The quasiparticle distribution function $n_\sigma(\mathbf{p}, T)$ has the well known Fermi-Dirac form

$$n_\sigma(\mathbf{p}, T, B) = \left\{ 1 + \exp \left[\frac{(\varepsilon_\sigma(\mathbf{p}, T) - \mu_\sigma)}{T} \right] \right\}^{-1}. \quad (3)$$

Here $\varepsilon_\sigma(\mathbf{p}, T)$ is the single-particle energy spectrum, μ is the chemical potential, being spin σ dependent due to the Zeeman splitting $\mu_\sigma = \mu \pm \mu_B B$, with μ_B is the Bohr magneton. The spectrum $\varepsilon_\sigma(\mathbf{p}, T)$ is obtained from the system energy $E[n_\sigma(\mathbf{p}, T)]$,

$$\varepsilon_\sigma(\mathbf{p}, T) = \frac{\delta E[n(\mathbf{p})]}{\delta n_\sigma}. \quad (4)$$

The effective mass $M^*(T, B)$ is given by [5, 6, 13].

$$\frac{1}{M^*(T, B)} = \frac{1}{m} + \sum_\sigma \int \frac{\mathbf{p}_F \mathbf{p}}{p_F^3} F(\mathbf{p}_F, \mathbf{p}) \frac{\partial n_\sigma(\mathbf{p})}{\partial p} \frac{d\mathbf{p}}{(2\pi)^3}. \quad (5)$$

Here, m is the free electron mass, $F(\mathbf{p}_F, \mathbf{p})$ is the Landau interaction, depending on momentum \mathbf{p} and the Fermi momentum \mathbf{p}_F . The main goal of the quasiparticle interaction $F(\mathbf{p}, \mathbf{p}_1)$ is to place the system at the topological FCQPT [5, 6]. Thus, the universal scaling behavior of HF metals can be explained, for it becomes independent of interactions near the formation of flat bands [5, 6]. Equations (3), (4) and (5) constitute the closed set that allows one to find $\varepsilon_\sigma(\mathbf{p}, T)$ and $n_\sigma(\mathbf{p}, T)$. In this case the effective mass is determined by the expression $p_F/M^* = \partial\varepsilon(p)/\partial p|_{p=p_F}$. At the topological FCQPT point, the analytical solutions of Eq. (5) are possible, see e.g. [5]. In contrast to the LFL theory with M^* being an approximatively constant parameter, here at zero magnetic field, M^* , exhibiting the NFL behavior, becomes temperature dependent. This feature represents the vivid deviation from the LFL picture, determining the NFL regime

$$M^*(T) \simeq a_T T^{-2/3}, \quad (6)$$

where a_T is fitting parameter. At raising temperatures and under the application of magnetic field B , the system undergoes a transition to the LFL behavior, so that the effective mass becomes approximately independent of T and $\rho(T) \propto T^2$, see Figs. 1, 3.

$$M^*(B) \simeq a_B (B - B_{c0})^{-2/3} \quad (7)$$

where a_B is fitting parameter. We recall that in case of CeCoIn₅ the critical field $B_{c0} \simeq 5.0$ T. In some cases as in the HF metal CeRu₂Si₂, $B_{c0} = 0$ [31], and in YbRh₂Si₂, $B_{c0} \simeq 0.07$ T [32]. It is seen from Eq. (6) that a HF metal located near FCQPT demonstrates the typical NFL behavior related to the strong dependency of M^* on T ,

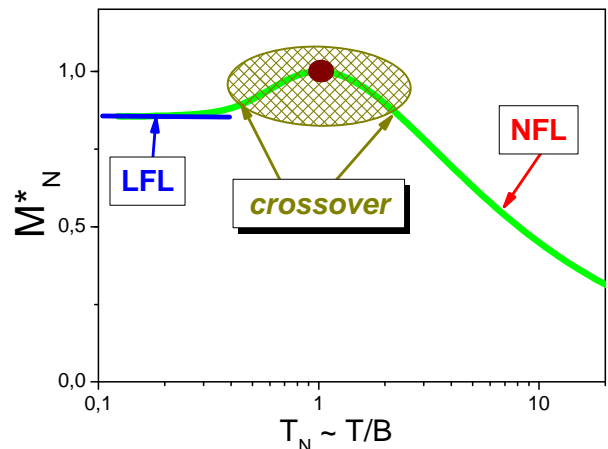


FIG. 5: (color online) Universal scaling behavior of the thermodynamic properties of HF metals defined by the normalized effective mass M_N^* . As follows from Eq. (10), under the application of magnetic field $T_N \propto T/(B - B_{c0})$, solid curve depicts M_N^* versus normalized temperature T_N . It is seen that at finite $T_N < 1$ the LFL behavior takes place. At $T_N \sim 1$ the system enters crossover state, and at elevating temperatures demonstrates the NFL behavior.

so that $M^*(T \rightarrow 0) \rightarrow \infty$. It follows from Eq. (7) that the application of B makes HF metal transits to the LFL state with $M^*(T)$ exhibiting the LFL behavior [5]. These both prominent features are not observed in the case of the Landau Fermi liquid where M^* is of the same order of magnitude as the bare mass [13].

Now we turn to the universal scaling behavior of M^* . The introduction of "internal" (or natural) scales greatly clarifies the problem of the scaling behavior. We first observe that near the topological FCQPT, both the effective mass $M^*(B, T)$ and the solution of Eq. (5) have the maximum M_M^* at a temperature $T_M \propto B$ [5].

It is convenient to measure the effective mass and temperature in the units M_M^* and T_M respectively [5], and we arrive at normalized effective mass $M_N^* = M^*/M_M^*$ and temperature $T_N = T/T_M$. Using the internal scales M_N^* and T_N allows us to reveal the universal scaling behavior, see Fig. 5, since M_N^* and T_N do not depend on the specific properties of HF metal, while M_M^* and T_M do [5, 6]. Near the topological FCQPT, the dependence $M_N^*(T_N)$ can be approximated by the universal interpolating function that describes the transition from LFL to NFL states, given by Eqs. (6) and (7), and represents the universal scaling behavior of M_N^* [5, 6]

$$M_N^*(y) \approx c_0 \frac{1 + c_1 y^2}{1 + c_2 y^{8/3}}. \quad (8)$$

Here $y = T_N = T/T_M$ and $c_0 = (1 + c_2)/(1 + c_1)$, where c_1 and c_2 are fitting parameters. The magnetic field B enters Eq. (5) only in the combination $\mu_B B/T$, making $T_M \sim \mu_B B$. As a result, we obtain from Eq. (8) that

$$T_M \simeq a_1 \mu_B (B - B_{c0}), \quad (9)$$

where a_1 is a dimensionless fitting parameter, see e.g. [33]. In this case, the variable y becomes $y = T/T_M \propto T/\mu_B(B - B_{c0})$. Equation (9) permits to assert that Eq. (8) gives the universal scaling properties of the effective mass $M_N^*(y)$. Thus, the thermodynamic functions measured at different field form a single function $M_N^*(T_N = y)$ [5]. Since T and B enter symmetrically in Eq. (8), it also manifests the scaling behavior of $M_N^*(B, T)$ as a function of T/B :

$$T_N = \frac{T}{T_M} = \frac{T}{a_1 \mu_B (B - B_{c0})} \propto \frac{T}{(B - B_{c0})} \propto \frac{(B - B_{c0})}{T}. \quad (10)$$

This universal scaling exhibited by M_N is also shown in Fig. 5. We note that Eqs. (8) and (10) allow one to describe the universal scaling behavior of HF metals, see e.g. [5, 6].

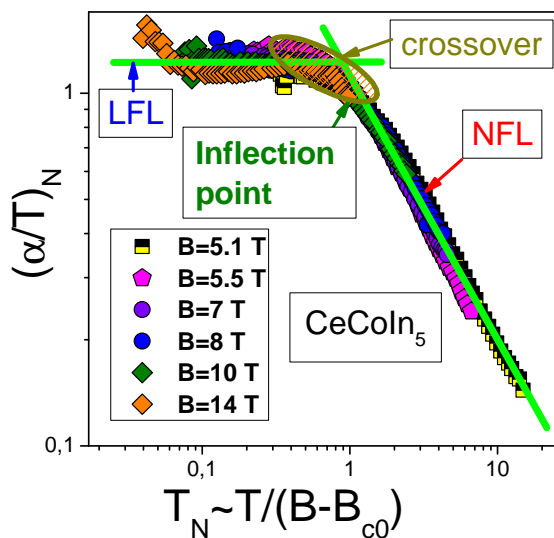


FIG. 6: (color online) Normalized low temperature thermal expansion coefficient $(\alpha/T)_N$ vs T_N at different B shown in the legend [28]. The data [34, 35] and T were normalized by the values of α/T and by the temperature $T_{inf} \simeq T_{cross}$, respectively, at the inflection point shown by the arrow. The horizontal solid line shows the LFL behavior, $(\alpha/T) = \text{const}$. The other solid line depicts the NFL behavior $(\alpha/T) \propto 1/T_N$.

Since the properties of HF metals are formed by the topological FCQPT inducing flat bands, see e.g. [5, 6], the behavior of the dimensionless thermal expansion coefficient of CeCoIn₅, treated as a function of the dimensionless temperature T_N , is also universal. Figure 6 shows that all the normalized data extracted from measurements on CeCoIn₅ [34, 35] collapse onto a single scaling curve [28]. As seen from the Fig. 6, the dimensionless coefficient $(\alpha(T, B)/T)_N$, treated as a function of T_N , at $T_N < 1$ shows a constant value, as depicted by the line, implying CeCoIn₅ exhibits the LFL behavior. At $T_N \simeq 1$ the system enters the narrow crossover region. At $T_N > 1$, the NFL behavior takes place, and $(\alpha/T)_N \propto 1/T_N$. From this observation we conclude that

the essential features of the experimental $T - B$ phase diagram of CeCoIn₅ are well represented by Fig. 1.

We now consider the differential tunneling conductivity $\sigma_d(V)$ between a HF metal and a simple metallic point. At low temperatures $\sigma_d(V)$ can be noticeably asymmetrical with respect to the change of voltage bias V that makes the asymmetrical part $\Delta\sigma_d(V) = \sigma_d(V) - \sigma_d(-V)$ finite. The asymmetry can be observed in experiments on HF metals whose electronic system has undergone the topological FCQPT, while the application of magnetic field causes the system to exhibit the LFL behavior, and eliminates the asymmetry, as has been predicted [15, 36]. Such a behavior has been observed in measurements on the HF metal CeCoIn₅ [37], displayed in Fig. 7. The data exposed in Fig. 7 have been extracted from [37], Fig. S17, and demonstrate the sample independence of the results. It is seen from Fig. 7, that $\Delta\sigma_d(V)$ is a linear function of V , and vanishes under the application of magnetic field that restores the LFL behavior [5, 14, 16, 36].

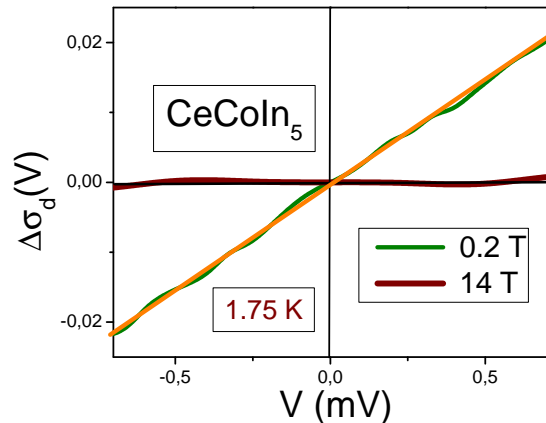


FIG. 7: (color online) Asymmetric part $\Delta\sigma_d(V)$ of the tunneling differential conductivity measured on CeCoIn₅ and extracted from the experimental data [37]. Linear dependence of $\Delta\sigma_d$ is shown by the straight line. The asymmetric part disappears at $B = 14$ T and $T = 1.75$ K, with $B_{c0} \simeq 5$ T.

Now consider how the presence of $\Delta\sigma_d(V)$ signals the violation of \mathcal{T} and \mathcal{C} symmetries [14, 15]. Suppose that we have a contact between HF and ordinary metals. Let us initially have the electronic current directed from HF metal to an ordinary one. Upon applying voltage V to the contact, we also change the electron charge $-e$ to $+e$ which alters immediately the current direction. Consequently, one obtains exactly the above electronic current under the voltage sign change $V \rightarrow -V$. As a result, the differential conductivity acquires the same asymmetric part $\Delta\sigma_d(V)$, as it is seen from Fig. 7. If \mathcal{C} were conserved, the asymmetrical part $\Delta\sigma_d(V) = 0$. Thus, we conclude that because of finite value of $\Delta\sigma_d(V)$ the \mathcal{C} symmetry is broken. Also, the substitution $t \rightarrow -t$ for constant charge generates the change of current direction only, where t is time. Since, the latter direction change can be accomplished by $V \rightarrow -V$ also, it is clear

that the time inversion symmetry is violated if $\Delta\sigma_d(V)$ is finite. Hence, both \mathcal{C} and \mathcal{T} symmetries are violated, provided that $\Delta\sigma_d(V) \neq 0$ emerges. Concurrently, the simultaneous transform $e \rightarrow -e$ and $t \rightarrow -t$ does not change anything, which means that combined \mathcal{C}, \mathcal{T} symmetry is preserved. It worth noting that in the present case the symmetry \mathcal{P} with respect to coordinates sign flip, that is the parity \mathcal{P} is not violated, so that the combined general $\mathcal{C}, \mathcal{P}, \mathcal{T}$ symmetry is kept intact [14, 15]. It is well known that both \mathcal{C} and \mathcal{T} symmetries are conserve for the systems of fermions, described by Landau theory. This implies that for these systems like ordinary metals $\sigma_d(V)$ is a symmetric function of its variable V , so that conductivity asymmetry $\Delta\sigma_d(V)$ is not observed in them at low T . As a result, in magnetic fields both the FC state and the asymmetry vanish, as soon as the LFL behavior is restored, see e.g. [5, 14, 15, 36]. We note that the application of magnetic field itself violates the \mathcal{T} symmetry, but this violation is rather weak to be observed in measurement of tunneling conductivity. Thus, $\Delta\sigma_d(V) \neq 0$ signals the presence of FC and the corresponding flat band that make the violation of both \mathcal{T} and \mathcal{C} finite [14, 15]. It is seen from Fig. 8 that CeCoIn₅ in its both the superconducting state and pseudogap one exhibits asymmetrical tunneling conductivity $\Delta\sigma_d(V) \neq 0$. The experimental data [38] displayed in Fig. 8 are in good agreement with the data obtained in Ref. [39], as it is shown in Ref. [40]. These facts confirm that beyond B_{c0} the FC state takes place, promoting both the superconducting and the corresponding pseudogap states [40]. It is seen from Fig. 8, that at $T \leq 2.7$ K $\Delta\sigma_d(V)$ is temperature independent, while CeCoIn₅ is in its superconducting and pseudogap states. Such a behavior is the intrinsic feature of HF metals located near the topological FCQPT [5, 16, 41]. We note that the violation of \mathcal{C} in strongly correlated Fermi systems was experimentally observed [42], as it was predicted [2, 5, 15, 36]. The interaction-driven violation of \mathcal{C} was observed in twisted bilayer graphene [43, 44]. Both this observation and the violation of \mathcal{T} in graphene support that the flat band of graphene is formed due to the topological FCQPT [14].

It is seen from the phase diagram 1 that at raising magnetic fields B and low temperatures T the HF metal CeCoIn₅ exhibits the LFL behavior and the symmetries are restored [14, 15]. The same behavior is exhibited by the HF metals YbRh₂Si₂ [45], YbCu_{5-x}Al_x (for $x=1.5$ [46]) and graphene [47], and explained within the framework of the FC theory [5, 40]. We note that the asymmetrical part $\Delta\sigma_d(V) \neq 0$ is observed in the normal state of HF metals without a change at $T \simeq T_c$, and diminishing when the the pseudogap vanishes, see Fig. 8 [5, 6, 46]. Under the application of magnetic field this asymmetry vanishes, thus possible in gap states in the superconducting state do not noticeably contribute to $\Delta\sigma_d(V)$. Again, we conclude that the phase transition in CeCoIn₅ is represented by the topological FCQPT and accompanied by the symmetry violation, as it does in the mentioned above HF metals and graphene.

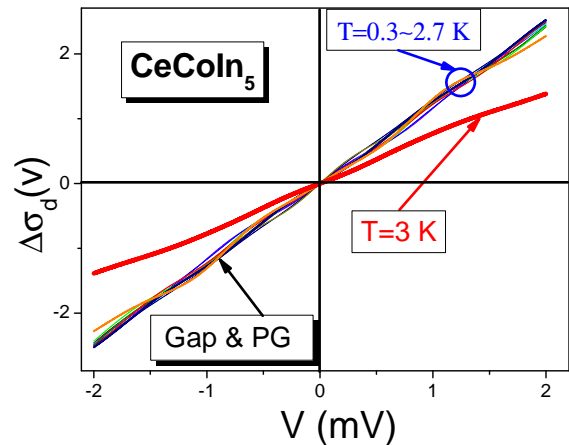


FIG. 8: (color online) The asymmetric part of tunneling conductivity $\Delta\sigma_d(V)$ in CeCoIn₅. $\Delta\sigma_d(V)$ is extracted from the experimental data [38]. At $2.3 \leq T \leq 2.7$ K CeCoIn₅ is in its pseudogap (PG) and at $T \leq 2.3$ in its superconducting states with $T_c = 2.3$ [38]. At $T \leq 2.7$ K, as it is shown by both the ring and the arrow, $\Delta\sigma_d(V)$ is temperature independent [5, 40, 41].

We are now in a position to consider in CeCoIn₅ a possible jump in the Hall coefficient at $B \rightarrow B_{c0}$ at the zero temperature limit. Measurements of the Hall resistivity $R_H(T, B)$ in external magnetic fields B versus T have revealed a diverse low-temperature behavior of this basic property in HF metals, ranging from the LFL behavior to the challenging NFL one [3, 5, 12].

It is instructive to compare the behavior of the Hall coefficient in archetypical HF metals CeCoIn₅ and YbRh₂Si₂. At $T \rightarrow 0$ in YbRh₂Si₂ the application of the critical magnetic field B_{c0} suppressing the antiferromagnetic phase (with the Fermi momentum $p_{AF} \simeq p_F$) restores the LFL behavior with the Fermi momentum $p_f > p_F$, making an abrupt change in the Hall coefficient $R_H(T \rightarrow 0, B \rightarrow B_{c0})$, as a function of B [5, 12]. At low temperatures and $B < B_{c0}$, the ground state energy of the antiferromagnetic phase is lower than that of the heavy LFL, while at $B > B_{c0}$ the opposite case takes place, and the LFL state wins the competition. At $B = B_{c0}$ both the antiferromagnetic and LFL states have the same ground state energy. Thus, at $T = 0$ and $B = B_{c0}$, the infinitesimally small change in the magnetic field B leads to the finite jump in the Fermi momentum. In response to this change, the Hall coefficient $R_H(B)$ undergoes the corresponding sudden jump [5, 9, 10, 12]. In the case of CeCoIn₅, one can hardly expect to observe such a jump, since QCP is hidden under the superconducting dome, see the phase diagram 1. As a result, one can only observe $R_H(B > B_{c0})$. Measurements of the Hall coefficient on CeCoIn₅ do not show the possible jump, while the observed temperature dependence of $R_H(T, B)$ [3] can be explained within the framework of the FC theory [48]. The absence of the jump in the Hall coefficient makes the illusion that the

quantum phase transition in CeCoIn_5 is not accompanied by the violation of symmetry, but the study of the \mathcal{T} and \mathcal{C} symmetries and the change of the residual resistivity ρ_0 clearly signals that the violation of the symmetry does take place.

In summary: We have delineated the quantum phase transition in CeCoIn_5 , and explained a number of experimental data collected in measurements on CeCoIn_5 . The

quantum phase transition in CeCoIn_5 is accompanied by the symmetry breaking and represented by the topological FCQPT that connects two Fermi surfaces of different topological charges and forms flat bands.

This work was supported by U.S. DOE, Division of Chemical Sciences, Office of Basic Energy Sciences, Office of Energy Research, AFOSR.

-
- [1] V.A. Khodel and V.R. Shaginyan, JETP Lett. **51**, 553 (1990).
- [2] V.A. Khodel, V.R. Shaginyan, and V.V. Khodel, Phys. Rep. **249**, 1 (1994).
- [3] N. Maksimovic, D.H. Eilbott, T. Cookmeyer, F. Wan, J. Rusz *et al.*, Science **375**, 76 (2022).
- [4] M. Vojta, Rep. Prog. Phys. **66**, 2069 (2003).
- [5] V.R. Shaginyan, M.Ya. Amusia, A.Z. Msezane, and K.G. Popov, Phys. Rep. **492**, 31 (2010).
- [6] M.Ya. Amusia and V.R. Shaginyan, *Strongly Correlated Fermi Systems: A New State of Matter*, Springer Tracts in Modern Physics Vol. **283** (Springer Nature Switzerland AG, Cham, 2020).
- [7] V.A. Khodel, J.W. Clark, and M.V. Zverev, Phys. Rev. B **102**, 201108(R) (2020).
- [8] G.E. Volovik, JETP Lett. **53**, 222 (1991).
- [9] S. Kirchner, S. Paschen, Q. Chen, S. Wirth, D. Feng *et al.*, Rev. Mod. Phys. **92**, 011002 (2020).
- [10] M. Taupin and S. Paschen, Crystals **12**, 251 (2022).
- [11] N. Regnault, Y. Xu, M.-R. Li, D.-Sh. Ma, M. Jovanovic *et al.*, Nature **603**, 824 (2022).
- [12] S. Paschen, T.Lühmann, S. Wirth, P. Gegenwart, O. Trovarelli *et al.*, Nature **432**, 881 (2004).
- [13] E.M. Lifshitz and L.P. Pitaevskii, *Statistical Physics*, Part 2, Butterworth-Heinemann (1999).
- [14] V.R. Shaginyan, A.Z. Msezane, V.A. Stephanovich, G.S. Japaridze, and E.V. Kirichenko, Phys. Scr. **94**, 065801 (2019).
- [15] V.R. Shaginyan, A.Z. Msezane, G.S. Japaridze, and V.A. Stephanovich, Symmetry **12**, 1596 (2020).
- [16] V.R. Shaginyan, A.Z. Msezane, and G.S. Japaridze, Atoms **10**, 67 (2022).
- [17] Q.Y. Chen, D.F. Xu, X.H. Niu, J.Jiang, R. Peng *et al.*, Phys. Rev. B **96**, 045107 (2017).
- [18] L. Howald, G. Seyfarth, G. Knebel, G. Lapertot1, D. Aoki, and J.P. Brison, J. Phys. Soc. Jpn., **80**, 024710 (2011).
- [19] J. Paglione, M. A. Tanatar, D. G. Hawthorn, E. Boaknin, R. W. Hill *et al.*, Phys. Rev. Lett. **91**, 246405 (2003).
- [20] J. Paglione, M. A. Tanatar, D. G. Hawthorn, F. Ronning, R. W. Hill *et al.*, Phys. Rev. Lett. **97**, 106606 (2006).
- [21] A. Bianchi, R. Movshovich, N. Oeschler, P. Gegenwart, F. Steglich *et al.*, Phys. Rev. Lett. **89**, 137002 (2002).
- [22] M. Kenzelmann, Th. Strässle, C. Niedermayer, M. Sigrist, B. Padmanabhan *et al.*, Science **321**, 1652 (2008).
- [23] M. Kenzelmann, S. Gerber, N. Egetenmeyer, J.L. Gavilano, Th. Strässle *et al.*, Phys. Rev. Lett. **104**, 127001 (2010).
- [24] F. Ronning, C. Capan, E.D. Bauer, J.D. Thompson, J.L. Sarrao, and R. Movshovich, Phys. Rev. B **73**, 064519 (2006).
- [25] K. Izawa, H. Yamaguchi, Y. Matsuda, H. Shishido, R. Settai, and Y. Onuki, Phys. Rev. Lett. **87**, 057002 (2001).
- [26] V.R. Shaginyan, A.Z. Msezane, V.A. Stephanovich, and E.V. Kirichenko, Europhys. Lett. **76**, 898 (2006).
- [27] V.A. Sidorov, M. Nicklas, P.G. Pagliuso, J.L. Sarrao, Y. Bang *et al.*, Phys. Rev. Lett. **89**, 157004 (2002).
- [28] V.R. Shaginyan, A.Z. Msezane, K.G. Popov, J.W. Clark, M.V. Zverev, and V.A. Khodel, Phys. Rev. B **86**, 085147 (2012).
- [29] H. Polshyn, M. Yankowitz, S. Chen, Y. Zhang, K. Watanabe *et al.*, Nat. Phys. **15**, 1011 (2019).
- [30] P. Aynajian, E. Neto, A. Gyenis, R.E. Baumbach, J.D. Thompson *et al.*, Nature **486**, 201 (2012).
- [31] D. Takahashi, S. Abe, H. Mizuno, D.A. Tayurskii, K. Matsumoto *et al.*, Phys. Rev. B **67**, 180407 (2003).
- [32] P. Gegenwart, Y. Tokiwa, T. Westerkamp, F. Weickert, J. Custers *et al.*, New J. Phys. **8**, 171 (2006).
- [33] V.R. Shaginyan, A.Z. Msezane, G.S. Japaridze, S.A. Artamonov, and Y.S. Leevik, Materials **15**, 3901 (2022).
- [34] J. G. Donath, F. Steglich, E. D. Bauer, J. L. Sarrao, and P. Gegenwart, Phys. Rev. Lett. **100**, 136401 (2008).
- [35] S. Zaum, K. Grube, R. Schäfer, E. D. Bauer, J. D. Thompson, and H. v. Löhneysen Phys. Rev. Lett. **106**, 087003 (2011).
- [36] V.R. Shaginyan, JETP Lett. **81**, 222 (2005).
- [37] K. Shrestha, S. Zhang, L.H. Greene, Y. Lai, R.E. Baumbach *et al.*, Phys. Rev. B **103**, 224515 (2021).
- [38] S. Wirth, Y. Prots, M. Wedel, S. Ernst, S. Kirchner *et al.*, J. Phys. Soc. Japan **83**, 061009 (2014).
- [39] W.K. Park, L.H. Greene, J.L. Sarrao, and J.D. Thompson, Phys. Rev. B **72**, 052509 (2005).
- [40] V.R. Shaginyan, A.Z. Msezane, G.S. Japaridze, V.A. Stephanovich, and Y.S. Leevik, JETP Lett. **108**, 335 (2018).
- [41] V.R. Shaginyan and K.G. Popov, Phys. Lett. A **361**, 406 (2007).
- [42] A. Gourgout, G. Grissonnanche, F. Lalibertè, A. Ataei, L. Chen *et al.*, Phys. Rev. X **12**, 011037 (2022).
- [43] P. Stepanov, Nat. Phys. **18**, 608 (2022).
- [44] A.K. Paul, A. Ghosh, S. Chakraborty, *et al.*, Nature Physics **18**, 691 (2022).
- [45] S. Seiro, L. Jiao, S. Kirchner, S. Hartmann, S. Friedemann *et al.*, Nat. Commun. **9**, 3324 (2018).
- [46] G. Pristàš, M. Reiffers, E. Bauer, A.G.M. Jansen, and D.K. Maude, Phys. Rev. B **78**, 235108 (2008).
- [47] Y. Cao, V. Fatemi, S. Fang, K. Watanabe, T. Taniguchi *et al.*, Nature (London, U.K.) **556**, 43 (2018).
- [48] V.A. Khodel, M.V. Zverev, and J. W. Clark, JETP Lett. **81**, 315 (2005).